I&EC research
Industrial & Engineering Chemistry Research

Article

pubs.acs.org/IECR

A New Process for Azeotropic Mixture Separation by Phase Behavior Tuning Using Pressurized Carbon Dioxide

Kongmeng Ye,[†] Hannsjörg Freund,*[,†,‡] and Kai Sundmacher[†,§]

[†]Max Planck Institute for Dynamics of Complex Technical Systems, Sandtorstr. 1, D-39106 Magdeburg, Germany
[‡]Chemical Reaction Engineering, Friedrich-Alexander-University Erlangen-Nürnberg, Egerlandstr. 3, D-91058 Erlangen, Germany
[§]Process Systems Engineering, Otto-von-Guericke University Magdeburg, Postfach 4120, D-39106 Magdeburg, Germany

ABSTRACT: A fundamental approach to separate azeotropic mixtures by tuning the phase behavior using pressurized CO_2 as a tunable solvent was studied. Following this new process concept, two process variants were put forward to separate aqueous pressure-insensitive and pressure-sensitive azeotropic mixtures. The two process variants were studied in process simulations, and the potential was evaluated by comparison with a conventional pressure-swing distillation process for the acetonitrile−water system. The new process shows significant potential to reduce the separation costs by 30.5% up to 68.9% for a broad variety of mixtures with water fractions in the range of $0.1 \leq x_{H_2O} \leq 0.9$. Thus, these results clearly indicate that the novel fundamental separation approach is a promising alternative to conventional processes for the separation of azeotropic mixtures.

1. INTRODUCTION

An interesting experimental phenomenon was discovered in the 1950s: homogeneous aqueous solutions of alcohols or other polar solvents can be split into two liquid phases by pressurized gases, so-called "salting-out" agents.[1,2] In this regard, CO_2 is one of the most popular "salting-out" agents.[3] The vapor−liquid equilibrium (VLE) phase behavior of CO_2 + liquid can be tuned into a vapor−liquid−liquid equilibrium (VLLE) phase behavior by pressurizing CO_2, and the transition occurs at the lower critical solution pressure (LCSP). The liquid splits into an organic-rich liquid phase and a water-rich liquid phase. If the pressure is increased further, the upper critical solution pressure (UCSP) may be reached. At this point the organic-rich phase merges with the gas phase (see Figure 1).[4]

In the past, quite a number of research works focused on the experimental investigations of such interesting thermodynamic phenomena, as reviewed, e.g., by Adrian et al.[3] Also, the hypothetical potential of applying "salting-out" agents for technical separation purposes in a chemical process has already been mentioned in several publications.[3,5−8] However, to the best of our knowledge, as of today there is no rigorous modeling and simulation study dealing with the prediction and evaluation of such a "salting-out" approach for technical relevant mixtures. In particular, there is no publication which applies the special phase behavior tuning using pressurized CO_2 in a technical separation process and quantitatively compares the separation costs with the conventional separation processes.

For this reason, in this work we focus on the validation of the fundamental idea to separate azeotropic mixtures by phase behavior tuning using pressurized CO_2 at the technical process level, and on the quantitative evaluation of the potential of the novel process. For clarification purposes, it should well be noted already at this point that the new process concept is based on the use of subcritical CO_2 only; thus it is not to be mixed up with extraction processes based on the application of supercritical CO_2. Two general process variants were put forward for separating pressure-insensitive and pressure-sensitive azeotropic systems (see section 2) and were finally validated for a specific technically relevant system, i.e., the acetonitrile (MeCN) + water (H_2O) system (see sections 3 and 4).

2. PROPOSED PROCESS CONCEPT

Pressure-swing distillation (PSD) is a suitable method for separating pressure-sensitive azeotropic mixtures, as it provides several advantages over conventional distillation processes, e.g. with regard to energy savings by heat integration and due to the fact that no additional substances (e.g., entrainers) are required.[9−11] The separation principle of the PSD process is that the azeotropic point can be shifted by means of pressure variation (see the PSD process in Figure 2, P1 for LP and P2 for HP), and then the mixture can be separated continuously.

The separation principle of the new approach proposed in this work is different compared to the PSD process (see Figures 3 and 4). At first, a feeding mixture of an organic component and water (F) is pressed into CO_2. Once sufficient CO_2 is dosed and the system lies in the three-phase area (VLLE area), the liquid is split into two liquids, L1 and L2. L1 is pressure-dependent (see the dotted line), but L2 is quite close to pure water and nearly pressure-independent. The vapor phase is almost pure CO_2. The two liquids can release CO_2 conveniently, and two CO_2-free liquids L1′ and L2′ are generated. According to the lever rule, once the azeotropic point (AP) lies between L1′ and L2′, then the two liquids can be purified using two additional conventional distillation columns. The condensates close to the AP are recycled. That is exactly the principle of process variant 1 (see Figure 3).

If, however, the AP is too close to one of the sides (either water side or organic side), then one of the distillation columns operates at very low efficiency due to the large recirculation ratio

Received: May 29, 2013
Revised: August 21, 2013
Accepted: September 26, 2013
Published: September 26, 2013

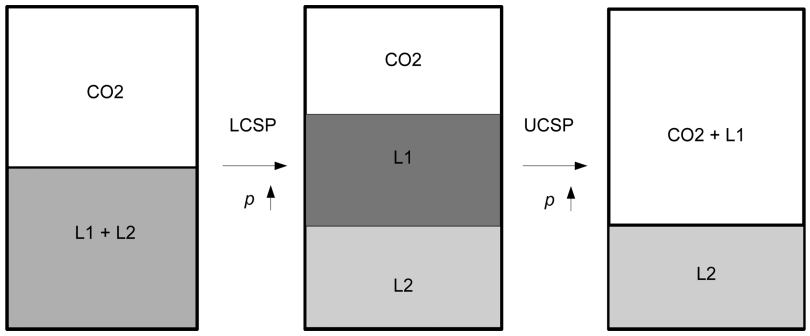

Figure 1. The phase changes observed upon expanding a mixture of two miscible liquids over a LCSP and an UCSP[4]

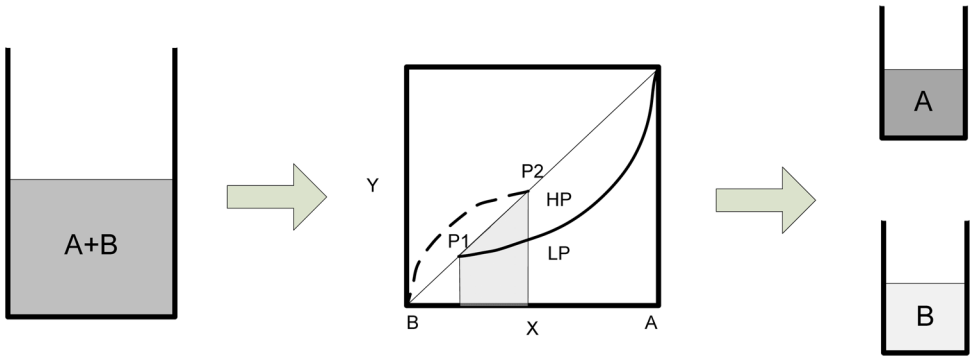

Figure 2. Separation principle of PSD.

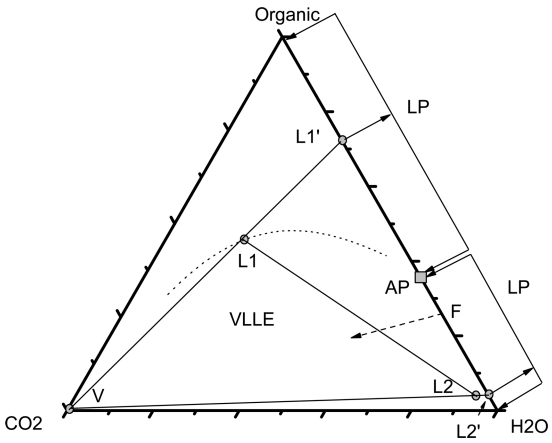

Figure 3. Separation principle of process variant 1.

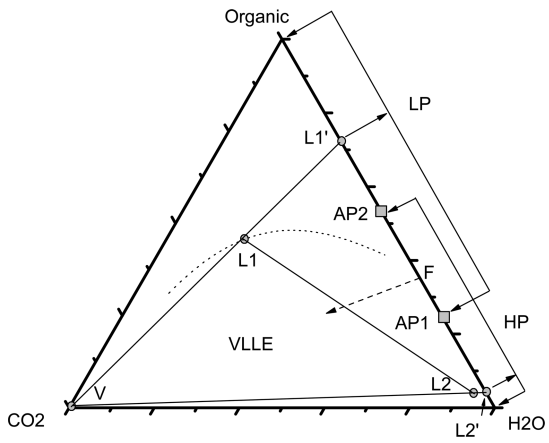

Figure 4. Separation principle of process variant 2.

of condensate according to the lever rule. For such a system, process variant 2 is beneficial. In Figure 4, the separation principle of process variant 2 is displayed. In this process, L1′ is separated in a low pressure (LP) distillation column. For L2′, a high pressure (HP) column is used to increase the distillation efficiency of separating L2′, because the AP2 under HP is shifted to another position, which is much farther away from L2′ than AP1 under LP. Therefore, the circulated azeotropic mixture will be reduced significantly according to the lever rule. In this way, process variant 2 couples the "salting-out" effect with the pressure impact on the pressure-sensitive azeotropic system.

3. CASE STUDY: SYSTEM AND MODELING

To evaluate the two proposed process variants described above, the technically relevant azeotropic system acetonitrile (MeCN) + water (H_2O) was selected. This system has been investigated in previous research work, and in several articles[9,12−15] it is stated that the PSD process is an appropriate method for the separation of MeCN and H_2O. Therefore, the system is a desirable choice for the case study from both a scientific and a practical point of view. The technical relevance of the system arises from the fact that acetonitrile is a widely used solvent in the chemical industries.

A rigorous thermodynamic modeling is the base of a reliable process simulation. Therefore, at first, the involved binary system (MeCN + H_2O) under atmospheric pressure and the ternary system (MeCN + H_2O + CO_2) under modest elevated pressure were modeled, which are described in following two sections.

3.1. Binary System. The VLE phase behavior of the MeCN + H_2O system was predicted by the Non-Random Two Liquids-Ideal Gas model (NRTL-IG), which had previously been successfully applied for this system as reported in the literature.[12,13] In this approach, the NRTL model is used for the description of the liquid phase, and the vapor phase is assumed as

ideal gas. The modeling steps and the performance of the model are highlighted in Appendix A.

3.2. Ternary System. In the open literature, there are only very few data available for the system MeCN + H_2O + CO_2. Lazzaroni et al.[16] report five points of experimental VLLE data, and they modeled the system using CEoS/GE models. CEoS/GE models are often applied for the simulation of the VLLE phase behavior of systems that involve pressurized CO_2.[3,4] On the basis of our previous experience in modeling such multicomponent systems with pressurized CO_2 which feature a complex phase behavior,[17,18] we prefer to use the PRWS model as a suitable representative of the CEoS/GE models for predicting the system. The detailed modeling steps and the performance of the model are illustrated in Appendix B.

3.3. Process Simulation. The proposed process variants and a conventional PSD process were simulated using the commercial process simulation software Aspen Plus (V7.1). The VLLE phase behavior of the MeCN + H_2O + CO_2 system was predicted for a constant temperature (40 °C) and modest pressures (pressure range 25−65 bar). For the simulation of the distillation, a rigorous equilibrium stage model was used.

Nine different feed compositions (x_{H_2O} = 0.1−0.9 mol/mol, increasing increment 0.1) were investigated to evaluate which composition range would have potential for the application of the new process variants. The feed flow was set to 6.4×10^5 kmol/a (i.e., 1.30×10^4 to 2.48×10^4 ton/a, depending on the feed composition), and the product qualities were specified to x_{MeCN} = 99.5% (mol/mol) and x_{H_2O} = 99.9% (mol/mol) for all cases.

4. RESULTS AND DISCUSSION

Since this work is focusing on evaluating the potential of a fundamental separation idea for a technical process, the capital costs are not considered at this point. Instead, the running separation costs as operational costs were evaluated. The costs of the used utilities are listed in Table 1.

Table 1. The Costs of Used Utilities[13a]

utility	quality	costs	purpose
electricity		0.084 (USD/kWh)	pumps and compressor
water	18−40 °C	0.06 (USD/ton)	cooling
steam 1	100 °C	17.00 (USD/ton)	heating: LP in PSD; LP in process variant 1
steam 2	120 °C	17.82 (USD/ton)	heating: LP in process variant 2
steam 3	150 °C	20.15 (USD/ton)	heating: HP in PSD; byproduct in process variant 2
steam 4	190 °C	26.68 (USD/ton)	heating: HP in PSD; HP in process variant 2

[a]Note: the steam prices are 0.02712−0.04860 USD/kWh (100°C −190°C), which are calculated according to the latent energy of steam. The electricity price is 1.7−3.1 times as expensive as steam with respect to the same energy (kWh).

Additionally, the recycle ratio of the mixture and CO_2 and the energy requirement for the separation (electricity and steam) were also calculated in process analysis using the following equations:

$$\text{separation costs (USD/kmol)} = \frac{\text{costs (USD/h)}}{\text{feed (kmol/h)}}$$

$$\text{recycle ratio} = \frac{\text{recycled mixture flow (kmol/h)}}{\text{feed (kmol/h)}}$$

$$\text{energy requirement (kWh/kmol)} = \frac{\text{duty (kW)}}{\text{feed (kmol/h)}}$$

Three terms, i.e., the electricity costs due to compression of recycled CO_2, the costs due to steam consumption, and the costs due to consumption of cooling water, were considered as contributing terms to the total separation costs.

4.1. PSD. The schematic flowsheet of the conventional PSD process is displayed in Figure 5, and the corresponding $y-x$ diagram of the MeCN + H_2O system is given in Figure 6. The specifications for the simulation of the conventional PSD process for two scenarios are listed in Table 2. The flowsheet of the process is illustrated for one case: for scenario 1, the feed is between 0 and AP2 in the $y-x$ diagram (see Figure 6), and the HP distillation can be used to separate the mixture into MeCN and P2. Then, P2 is sent to LP distillation, and P1 and H_2O are obtained. P1 is recycled as the internal flow of the whole system.

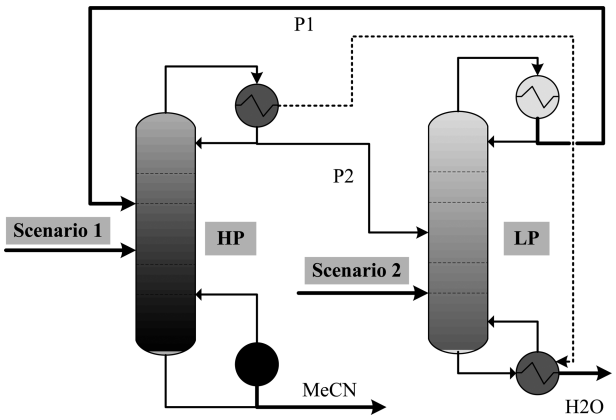

Figure 5. Scheme of the conventional PSD process for minimum-boiling azeotropic mixture separation.

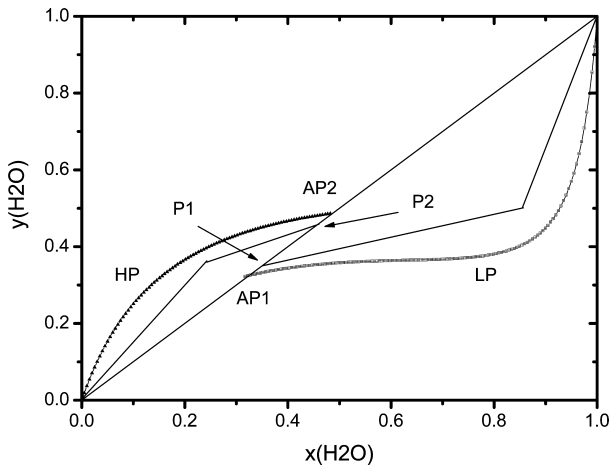

Figure 6. Operation of the conventional PSD process in a $y-x$ diagram.

Table 2. Specification of PSD Simulation

terms	specification
HP	10 bar, 30 stages
LP	1.01 bar, 30 stages
scenario 1 and streams	$x_{H_2O} \leq 0.4$; 15 (feed), 5 (P1), 5 (P2)
scenario 2 and streams	$x_{H_2O} > 0.4$; 20 (feed), 5 (P2), 10 (P1)

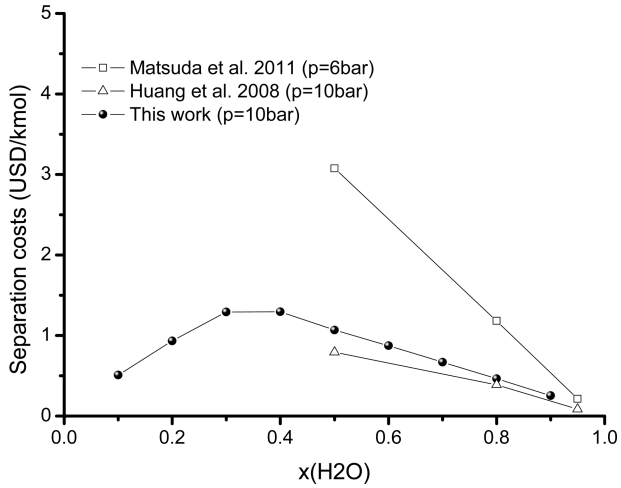

Figure 7. Separation costs of the PSD process in this work compared to literature data.[12,13]

Figure 7 displays the separation costs in dependence on the feed composition. Apparently, the pressure has a strong impact on the separation costs, which is in accordance with reference results.[12,13] The calculated separation costs of Matsuda et al.[13] are significantly higher than the result of this work and of Huang et al.,[12] because the pressure shift range in the first work is smaller (1−6 bar) in comparison with the range considered in the latter works (1−10 bar). As a consequence, the azeotropic point shift range is smaller, which in turn results in a larger recycle of the condensate and causes higher costs. The simulation results for the conventional PSD process in this work are realistic, as has been shown by comparison with the results of Huang et al.,[12] though the separation costs are slightly higher. For this there are two reasons: At first, Huang et al.[12] applied a more detailed heat integration technology in their specific PSD process. Second, the product stream purity in this work is higher than in the case of Huang et al.,[12] which is connected with higher energy demand.

Additionally, Figure 7 illustrates a clear tendency: The separation costs are increasing at first by increasing x_{H_2O} in the feed mixture. At x_{H_2O} = 0.3−0.4, the costs keep almost stable, and then they go down for x_{H_2O} > 0.4. The results of Huang et al.[12] also confirm such a tendency for the range x_{H_2O} = 0.5−0.95. The reason for this is that the range x_{H_2O} = 0.3−0.5 is the azeotropic point shift range. Consequently, the distillation operational costs are higher due to higher energy demand for the increased recycle ratio of the distillation condensate.

4.2. Process Variant 1 and Process Variant 2. The specifications of the two novel process variants are listed in Table 3. The schematic flowsheets are shown in Figures 8 and 9, respectively, while the corresponding operation of the two process variants in $y-x$ diagrams is displayed in Figures A5 and A6 (Appendix C).

The flowsheet of process variant 1: For scenario 1 (see Figure 8), raw feed mixture is fed into D1 (LP) to obtain the condensate mixture and MeCN at first, since the water fraction (x_{H_2O}) is too low so that the organic cannot be directly "salted-out" from the feed mixture. Then, the condensate mixture is compressed with CO_2, and the liquid is split into L1 and L2. Finally, L1 and L2 are sent to D1 (LP) and D2 (HP) in order to obtain pure MeCN and H_2O. The condensate mixtures are recycled again. In D2, a pressure of 3 bar is applied in order to enable heat integration between D1 and D2, which can reduce a part of the energy costs. For scenario 2, the raw feed mixture is fed and compressed with CO_2 directly. For scenario 3, the raw feed mixture is fed into D2 at first.

Table 3. Specification of Simulation of the Two Process Variants[a,b,c,d]

term	specification
process variant 1	scenario 1: $0 < x_{H_2O} \leq 0.2$; scenario 2: $0.3 \leq x_{H_2O} < 0.9$; scenario 3: $0.9 \leq x_{H_2O} < 1$
	D1: LP, 1.01 bar; D2: HP, 3.0 bar
process variant 2	scenario 1: $0 < x_{H_2O} < 0.3$; scenario 2: $0.3 \leq x_{H_2O} \leq 0.9$; scenario 3: $0.9 < x_{H_2O} < 1$
	D1: HP, 10 bar; D2: LP, 1.01 bar
D1, D2	30 stages, feed stage 10, RadFrac module, Murphree efficiency of all stages = 0.4
F1	25−65 bar (increase increment 5 bar), 40 °C (isothermal operation)
F2, F3, F4	ideal flash, 1.01 bar, 40 °C
P1	isentropic compressor, three stages
	outflow pressure setting is dependent on the pressure in F1
P2	liquid pump, pump efficiency = 0.95, drive efficiency = 0.95
	outflow pressure setting is dependent on the pressure in F1
C1, C2	cooler, 40 °C (outflow), isobaric
turbine	isentropic turbine, isentropic efficiency = 0.8, mechanical efficiency = 0.95, outflow pressure = 1.01 bar

[a]Three scenarios were used in order to cover wide feed composition ranges. The operation range is determined by the "salting-out" performance and the azeotropic points. [b]The boundary of "salting-out" performance is around x_{H_2O} = 0.2−0.3 (lower boundary), x_{H2O} = 0.9 (upper boundary). So in the range of x_{H_2O} = 0.3−0.9, the mixture can be split directly. [c]For the mixture with x_{H_2O} < 0.3 or x_{H_2O} > 0.9, it is not reliable to use pressurized CO_2. Thus, the feed needs to be distillated at first. [d]Process variant 1 did not cover the composition range with 0.2 < x_{H_2O} < 0.3, because the x_{H_2O} range was very close to the azeotropic point (x_{H_2O} = 0.3218, 1.01 bar) and the lower boundary of "salting-out" performance. In this range, the process potential was very small by either scenario 1 or scenario 2. However, process variant 2 was not limited in this range, because the azeotropic point was shifted to x_{H_2O} = 0.4867 under 10 bar.

The flowsheet of process variant 2 is very similar compared to process variant 1. The evident difference is that with two columns an opposite pressure-swing strategy is applied. D1 (HP) and D2 (LP) are applied to separate L1 and L2 (see Figure 9).

Since the release of pressurized CO_2 out of the liquids involves a decompression step, a fraction of the decompression energy can be recovered and used, e.g., for driving a turbine. Therefore, in order to check the potential of the cost reduction, both process variants were investigated for both subcases, with a turbine and without a turbine.

4.3. Results. To explain the key results systematically out of the huge amount of simulation results obtained, an overview of the separation costs is shown at first to choose an appropriate direction. Then, more details related to the process performance are given, and reasons are discussed and analyzed. This section is focusing on exhibiting the potential, the performance, and the "know-how" of the new process variants.

Figure 10 shows an overview on the separation costs reduction contrasting the conventional PSD process and the two novel process variants (for the case with the minimum separation costs among all investigated pressures).

Two important results can be summarized. First, the trend of the separation costs in the two process variants is similar, and

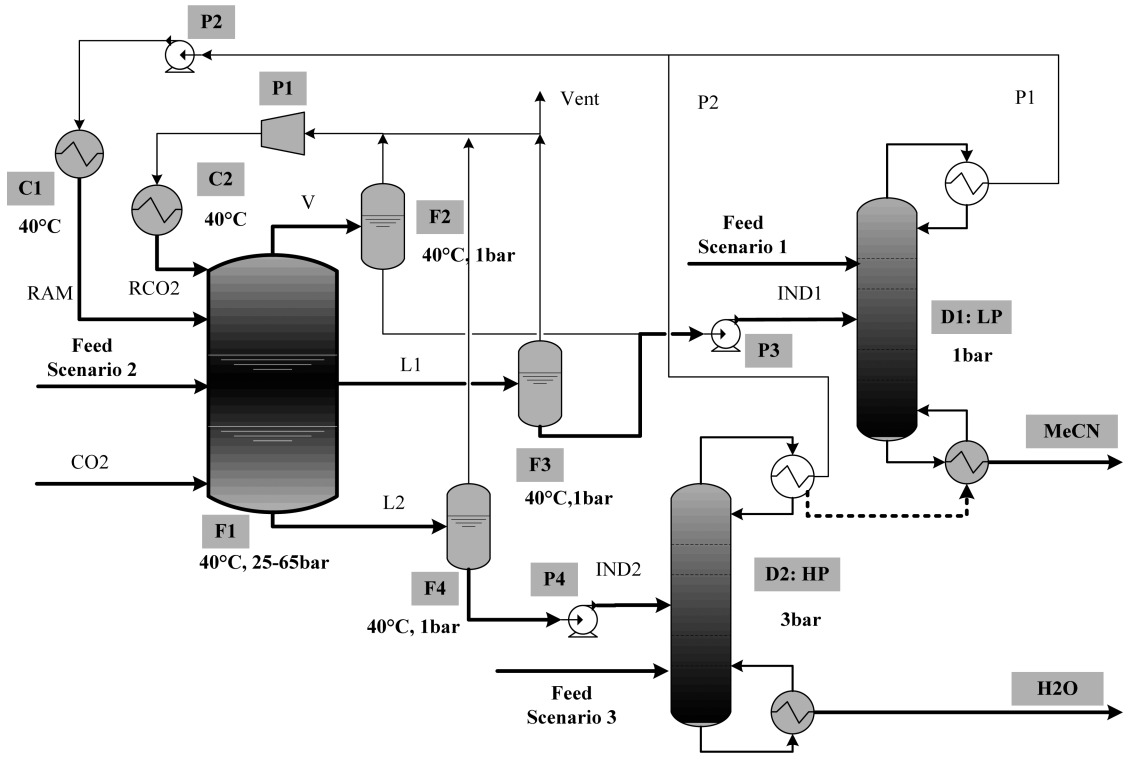

Figure 8. Schematic flowsheet of process variant 1.

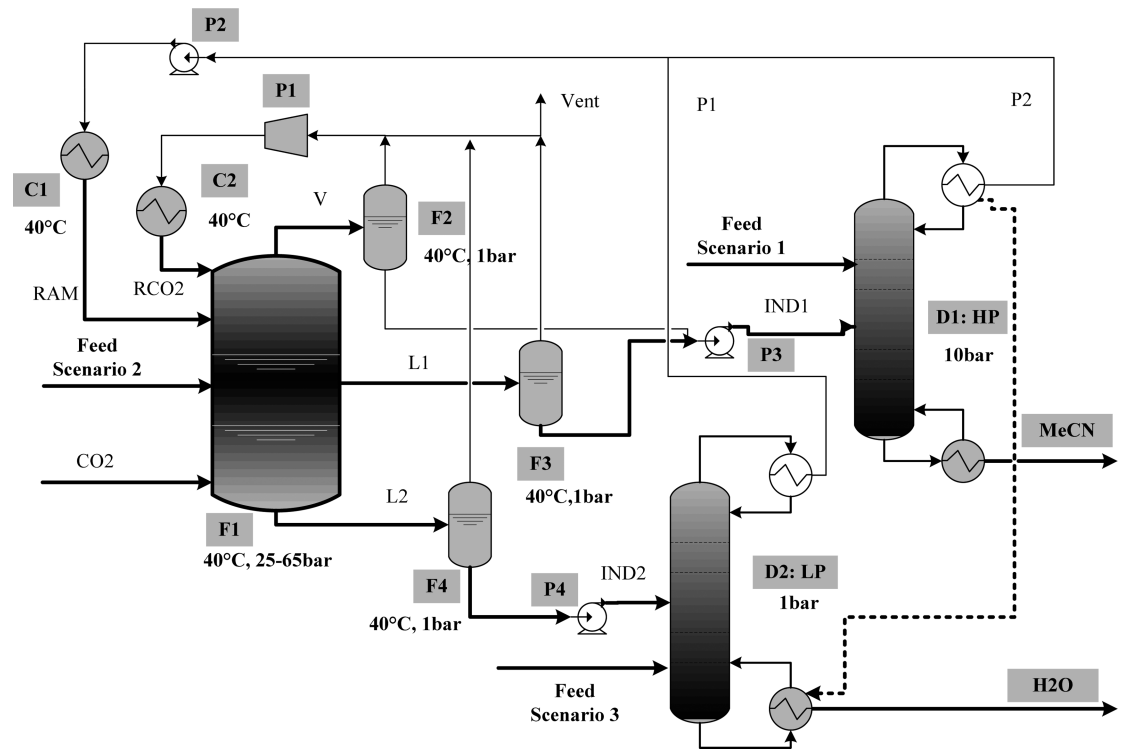

Figure 9. Schematic flowsheet of process variant 2.

both are lower compared to the conventional PSD process for almost all cases. This indicates that both of the new process variants generally have the potential to cut down the separation costs based on conventional PSD. The process variant 1 offers a cost reduction of 23.8−53.5% for the feed composition range of $0.3 \leq x_{H_2O} \leq 0.9$. With process variant 2, a cost reduction of 30.5−68.9% can be realized for a feed composition range of $0.1 \leq x_{H_2O} \leq 0.9$. At lower water fractions in the feed ($x_{H_2O} \leq 0.2$), however, process variant 1 features only very little cost reduction potential (at $x_{H_2O} = 0.2$), and even higher costs are involved at $x_{H_2O} = 0.1$. Therefore, process variant 2 is superior to process variant 1 with respect to the separation costs.

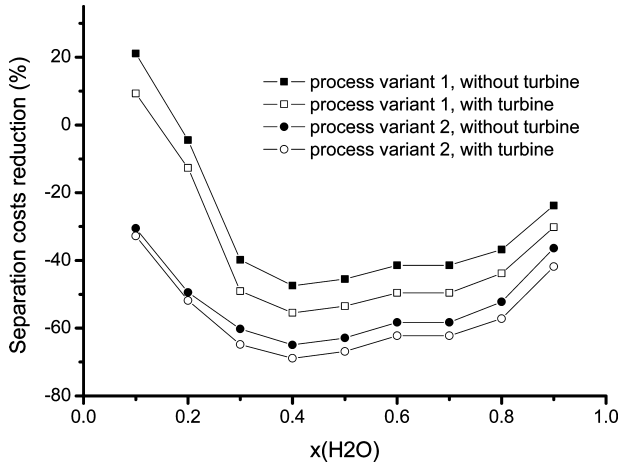

Figure 10. Separation cost reduction of the new process based on the conventional PSD process.

As a second important result, the profiles of the separation costs with and without turbine have no evident difference. This indicates that the application of a turbine does not affect the energy costs significantly; it can only save less than 5% for process variant 2 in general.

As for all the investigated cases in this work, the performance with and without a turbine is similar; the results of the process variant subcases with a turbine are not further discussed in the following. While both process variants show a similar qualitative performance, process variant 2 features a quantitatively better performance than process variant 1. Thus, the following text only discusses the results of process variant 2, while the results of process variant 1 are not investigated in detail.

If details in the process performance are investigated, then another very important point can be found (Figure 11): the

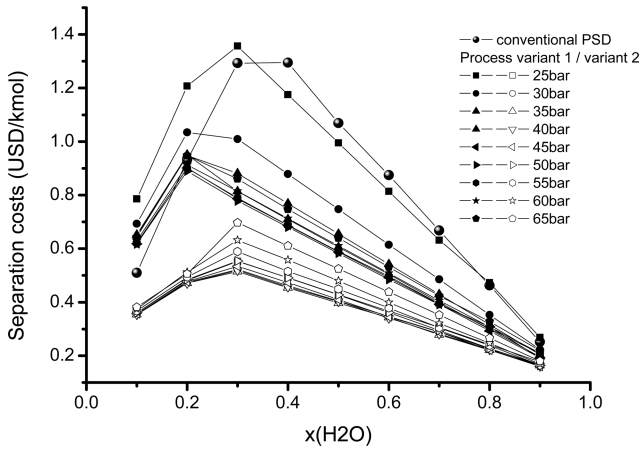

Figure 11. Separation costs dependent on operation pressure.

operating pressure of the VLLE flash, namely the operating pressure in short in the following text, has a big influence on the separation costs (for a fixed feed composition).

Figure 12 shows the operating pressure influence on the separation costs of process variant 2. Clearly, there is an optimal operating pressure range between 35 and 45 bar. This diagram indicates that the process is in fact dominated by the operating pressure. This can be illustrated by the two main contribution terms, i.e. the recycled CO_2 flow and the recycled condensate

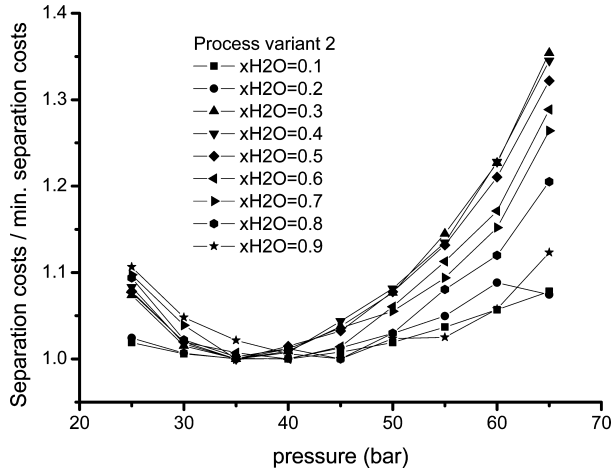

Figure 12. Operating pressure influence on normalized separation costs of process variant 2.

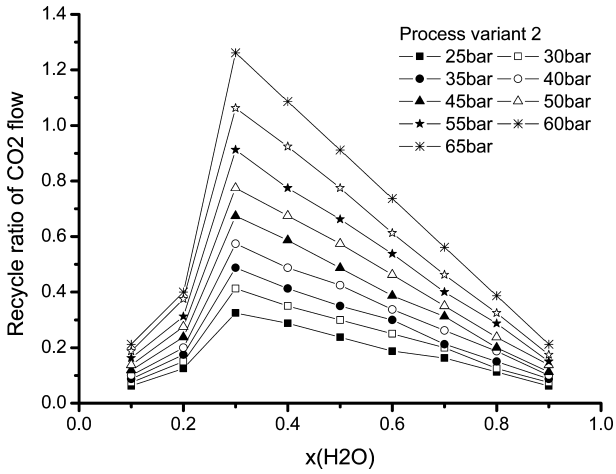

Figure 13. Recycle ratio of CO_2 flow in process variant 2.

mixture flow, which contribute to the separation costs in terms of electricity and heating energy consumptions, respectively.

Figure 13 displays the recycle ratio of CO_2 flow in process variant 2. The figure indicates that the operating pressure has a positive impact on the recycled CO_2 flow. For example, the recycled CO_2 flow is increased by a factor of 3−4 when the pressure rises from 25 to 65 bar at $x_{H_2O} = 0.3$. This dominant influence of the operating pressure has a very clear physical background: the higher the operating pressure, the more CO_2 can be pressed into the liquid.

Of course, more electricity is needed to compress more CO_2 and to provide and maintain the higher pressure level compared to the conventional PSD process. Figure 14 highlights the electricity requirement of process variant 2. The electricity requirement can increase by a factor of 4−5 when the operating pressure is increased from 25 to 65 bar. This trend is quantitatively similar to the increase of the recycle ratio of the CO_2 flow. Obviously, the operating pressure has a direct impact on the CO_2 flow, and both the operating pressure as well as the CO_2 flow have a positive influence on the electricity requirement.

As observed above, process variant 2 inevitably requires more electricity in comparison with the conventional PSD process due to more CO_2 compressing. Thus, at first it seems astonishing that process variant 2 still offers significant potential to reduce the

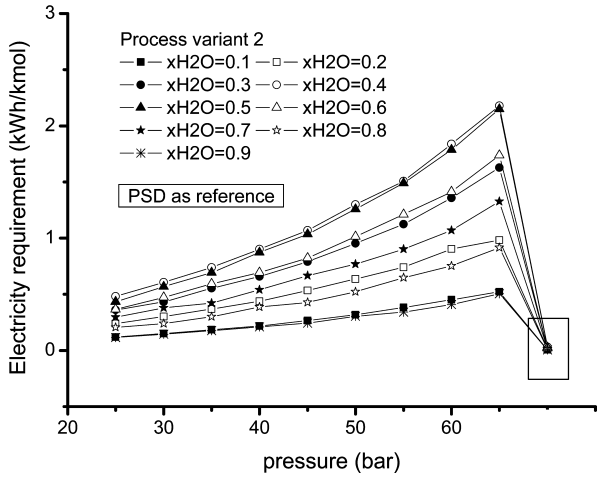

Figure 14. Electricity requirement of process variant 2.

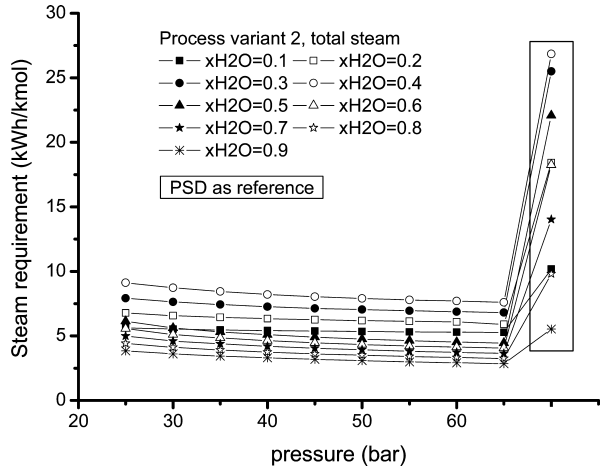

Figure 16. Steam requirement of process variant 2.

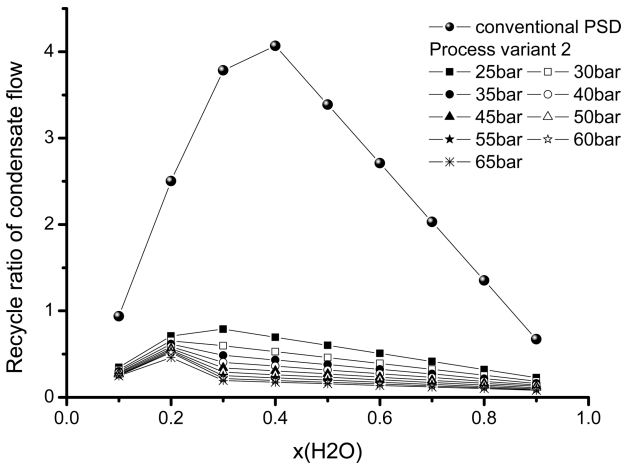

Figure 15. Recycle ratio of condensate flow in process variant 2.

separation costs. The reason for this is caused by another key factor: the reduction of the condensate recycle flow.

Figure 15 illustrates the significant reduction of the recycle ratio of the condensate flow in process variant 2 compared to conventional PSD. This huge reduction can be attributed to the synergistic effects resulting from the "salting-out" performance and the pressure-swing strategy. The minimum reduction is 73.6%, and the maximum reduction achieves 95.7% for the best case among all feed composition ranges. All the best cases for each feed composition are the ones at the highest investigated pressure (65 bar), which indicates that the high operating pressure can enhance the "salting-out" performance. By increasing the distance of the two liquids in the composition space, the distillation and thereby the separation efficiency of the whole process can be significantly improved. As a consequence, the total recycled condensate mixture flow reduces. This significant flow reduction provides several benefits to the distillation. On the one hand, the total steam requirement for heating is reduced, which can be seen directly in Figure 16. Additionally, the required size of the columns is reduced, which will result in a significant reduction of the capital costs. For a clear understanding of the behavior of the proposed process, two tables (Tables 4 and 5) containing information on the flows and distillation columns are added.

The analysis above reveals the inherent reason for the optimal operating pressure range in Figure 12. The opposite impacts of the operating pressure on the electricity requirement and the steam requirement give rise to an arc-shaped performance curve in Figure 12. The electricity requirement is only around one-tenth of the steam requirement (Figures 14 and 16), but the costs for electricity are much higher than for steam with respect to the same energy amount (see utility costs in Table 1). Therefore, the separation costs are dominated by steam only in the low pressure range, while for higher pressures the electricity is increasingly dominating the separation costs.

4.4. Discussion. The previous discussion of the detailed results in the case study can be summarized and generalized. It should be noted that the novel separation concept is very flexible and can in principle easily be transferred to other pressure-sensitive systems. Thus, the two proposed process variants are not limited to the specific MeCN + H_2O system investigated in this work but can be considered as general separation approaches. In a number of additional studies, we have successfully applied the concept for, e.g., the separation of the 1,4-dioxane + water system and the propanol + water system.

Of course, the novel separation concept is not advantageous under all circumstances. Once the azeotropic system is extremely asymmetric and the azeotropic point does not lie between L1 and L2 any longer (Figure 2), then the addition of CO_2 cannot salt out the organic fraction. Therefore, this separation approach is not suitable for this system class and nonaqueous azeotropic mixtures. Thus, it has to be considered that the potential field of application of this novel separation approach is different compared to PSD or other existing technologies for separating azeotropic mixtures due to the specifics of the fundamental separation principle.

The feed composition considered in this study varies in a broad range, which yields a large variation with regard to the size of equipment. In this fundamental study, it is not yet the aim to estimate capital costs quantitatively. However, a qualitative analysis can be carried out at this point. The new process variants at a first glance have several disadvantages; e.g., they require a higher number of equipment components (including flash tanks, coolers, and compressors), a thicker (or more expensive) tank, and better sealing technology due to the elevated pressure, and also a more complex control system compared to the conventional PSD process. However, the significant reduction of the recycled condensate stream (e.g., 73.6–95.7% reduction for process variant 2) also decreases the size of all components drastically, in particular the distillation columns. This significant

Table 4. Detailed Information on the Flows for an Exemplified Case[a,b]

	feed	CO2	P2	P1	RCO2	RV1	RV2	RV3	L1	L2
T, °C	39.9	39.9	158.4	76.4	40	40	40	40	40	40
flow, kmol/h	80.00	0.03	21.44	3.92	34.00	1.62	32.00	0.42	61.60	43.76
mole fraction										
H_2O	0.50		0.45	0.34					0.16	0.94
MeCN	0.50		0.55	0.66					0.84	0.06
CO_2		1.00			1.00	1.00	1.00	1.00		

[a]The information on this table is for a case with these conditions: process variant 2, $x_{H_2O} = 0.5$, $p = 40$ bar. [b]The losses of acetonitrile and water are not considered in this work based on the small vent of CO_2 and low solubility of acetonitrile and water in CO_2 at 1.01 bar.

Table 5. Detailed Information on the Columns for an Exemplified Case Compared to PSD[a]

	PSD	process variant 2
D1 (HP)	10 bar	10 bar
reflux ratio	0.0600	0.3499
distillate rate, kmol/h	155.62	21.44
bottoms rate, kmol/h	39.84	40.16
cooler, MW	−1.5491	−0.2422
reboiler, MW	1.3530	0.5348
D2 (LP)	1 bar	1 bar
reflux ratio	0.0900	0.6030
distillate rate, kmol/h	115.46	3.92
bottoms rate, kmol/h	40.16	39.84
cooler, MW	−1.0599	−0.0589
reboiler, MW	1.4737	0.1141

[a]The information in this table is formulated from the case with these conditions: PSD, $x_{H_2O} = 0.5$; process variant 2, $x_{H_2O} = 0.5$, $p = 40$ bar.

improvement counteracts all the disadvantages of the new process concept concerning the total capital costs because the distillation columns are usually a main factor, being much more expensive than other equipment components.

In process variant 2, the synergistic effect generated by the "salting-out" performance and the pressure-swing strategy strongly enhances the separation efficiency. This combination is a very flexible option and can help to overcome some particular problems. For example, with process variant 1 and with the conventional PSD process a. the feed mixture $x_{H_2O} = 0.3$ cannot be separated economically, because this feed location is too close to the location of the azeotropic point (under LP) and one side of the "salting-out" liquid phases. With process variant 2, in contrast, this problem can be overcome.

Obviously, it cannot be concluded that process variant 2 always shows a better performance than process variant 1 for other systems. The system MeCN + H_2O is just one example that has been chosen, since it is a system of technical relevance and at the same time a suitable reference as data in the open literature is available. This system is an asymmetric system; i.e., the azeotropic point is close to the MeCN side under low pressure. For such systems, process variant 2 provides a benefit with respect to a larger reduction of the recycled condensate stream to higher pressure distillation in comparison with process variant 1 according to the lever rule. However, once the azeotropic properties are different in other systems, the required higher quality steam and the higher capital costs for the HP column might counterbalance the advantage of process variant 2. For this reason, it is necessary to reconsider the potential of both the process variants for each specific system with regard to the "salting-out" performance and the influence of the property of azeotropic point shift. Especially for some pressure-insensitive systems, process variant 1 may still be an attractive alternative compared to process variant 2.

Finally, it should be noted that CO_2 is a well-known benign solvent,[4,19−21] which is an interesting alternative compared to the conventional organic solvents. Considering the negative environmental impact of many of the traditional organic solvents that are used, a wide application range, and on a large scale, the new separation technology presented in this work using the near-/subcritical CO_2 as a benign solvent seem very attractive and maybe help to pave the way toward more sustainable separation processes.

5. CONCLUSION

In this work, a new process concept is proposed for azeotropic mixture separation by phase behavior tuning using pressurized CO_2. Two process variants were developed and validated by means of process simulation studies for the MeCN + H_2O system, and the performance of the two process variants was evaluated. The results were compared to that of the technical reference process scheme, i.e., a conventional PSD separation process. The major findings can be summarized as follows:

- Process variant 2, which combines the "salting-out" performance and pressure-swing strategy, shows the best potential with savings in the separation costs of 30.5−68.9% compared to the conventional PSD process for a feed mixture in the range of $0.1 \leq x_{H_2O} \leq 0.9$. With process variant 1, a reduction of 23.8−53.5% in the separation costs for a feed mixture range of $0.3 \leq x_{H_2O} \leq 0.9$ was achieved.
- The significant reduction of the recycled condensate stream is the primary contribution to the separation costs saving. With process variant 2, the recycled condensate stream can be reduced by 73.6−95.7%.
- The operating pressure of the VLLE flash has a qualitatively similar arc-shaped influence on the separation costs for both process variants. The counteracting impact of the operating pressure on the electricity requirement and the steam requirement results in an arc-shaped performance curve.
- As a result, there exist optimal operating pressure ranges. For process variant 2, the optimal pressure range is 35−45 bar.

6. APPENDIX

Appendix A. NRTL Model

$$\ln \gamma_i = \frac{\sum_{j=1}^{N} x_j \tau_{ji} G_{ji}}{\sum_{k=1}^{N} x_k G_{ki}} + \sum_{j=1}^{N} \frac{x_j G_{ij}}{\sum_{k=1}^{N} x_k G_{kj}} \left(\tau_{ij} - \frac{\sum_{m=1}^{N} x_m \tau_{mj} G_{mj}}{\sum_{k=1}^{N} x_k G_{kj}} \right)$$

$$\text{with } \tau_{ij} = a_{ij} + \frac{b_{ij}}{T/K}, \; G_{ij} = \exp(-\alpha \tau_{ij})$$

The NRTL parameters of the system MeCN + H_2O are listed in Table A1.

The performance of the NRTL-IG model for the system is demonstrated in Figures A1 and A2. The two figures indicate that

Table A1. NRTL Parameters[a]

compd. i	compd. j	a_{ij}	a_{ji}	b_{ij}	b_{ji}	α
H_2O	MeCN	1.0567	−0.1164	283.4087	256.4588	0.3

[a]Note: The NRTL parameters are from Aspen Internal Database (V7.1)

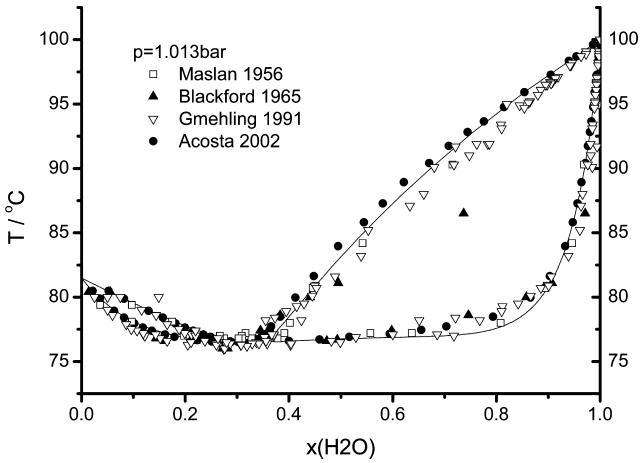

Figure A1. $T-x$ diagram of H_2O + MeCN binary system (1.013 bar). Data references 22−25.

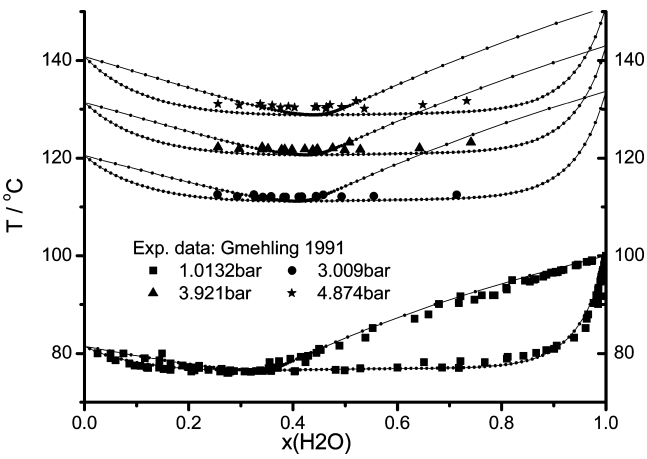

Figure A2. $T-x$ diagram of H_2O + MeCN binary system under different pressures 1.0132−4.874 bar. Data reference 24.

the NRTL-IG model predicts the VLE phase behavior of the MeCN + H_2O system well within a pressure range between 1 and 5 bar. According to literature,[12,13] the NRTL-IG model is reliable for predicting the VLE phase behavior of the MeCN + H_2O system up to 10 bar. Therefore, in this work, the NRTL-IG model was also used to predict the VLE phase behavior up to 10 bar. Figure A3 demonstrates the pressure-sensitive azeotropic point shift from 1.01 to 10 bar. The azeotropic points under 1.01 bar and 10 bar have a water content of x_{H_2O} = 0.3218 and x_{H_2O} = 0.4867, respectively.

■ APPENDIX B. PRWS MODEL

The PRWS modeling steps are the same as communicated in our previous publication.[17] The properties of the substances for the

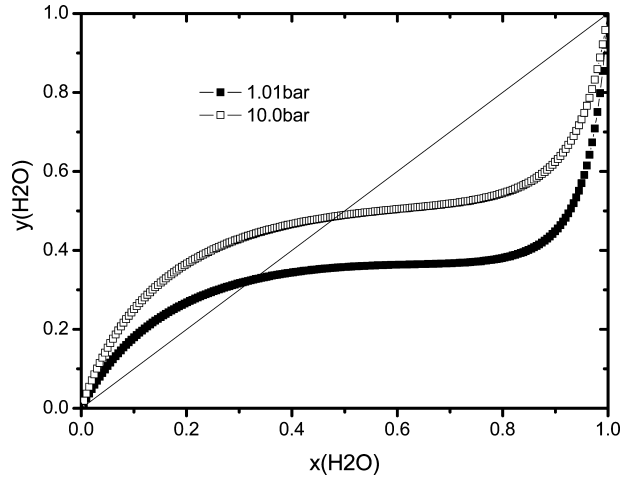

Figure A3. Sensitivity of the azeotropic point of the MeCN + H_2O system on pressure variation, predicted by the NRTL-IG model.

Table A2. Properties of Chemicals Used in PR EoS[a]

component	H_2O	CO_2	MeCN
ω	0.344 861	0.223 621	0.337 886
P_C/bar	220.55	73.83	48.3
T_C/°C	373.98	31.06	272.35

[a]Note: the data are from Aspen Internal Database (V7.1).

PR EoS are listed in Table A2. The interaction parameters k_{ij} of the WS mixing rule were regressed using Aspen Properties (maximum likelihood method) based on literature data[16] and are displayed in Table A3. The UNIFAC-PSRK approach was used for calculating the activity coefficients, and the involved parameters are listed in Tables A4 and A5.

Table A3. Regressed k_{ij} of PRWS

compd. i, compd. j	$k_{i,j} = k_{j,i}$
H_2O, MeCN	0.371 976
H_2O, CO_2	0.783 218
MeCN, CO_2	0.548 554

Table A4. Chemical Decomposition and Group Parameters[26]

chemical	group	R	Q
CO_2	CO_2	1.3000	0.9820
H_2O	H_2O	0.9200	1.4000
MeCN	MeCN	1.8701	1.7240

Table A5. Group Interaction Parameters[26]

group m,n	H_2O	MeCN	CO_2
H_2O	0	112.6	−1163.5
			5.4765
			−0.002 603
MeCN	242.8	0	307.1
CO_2	1720.6	−231.3	0
	−4.3437		
	0.001 31		

The performance of the PRWS model is demonstrated in Figure A4 (the predicted line within a pressure range between

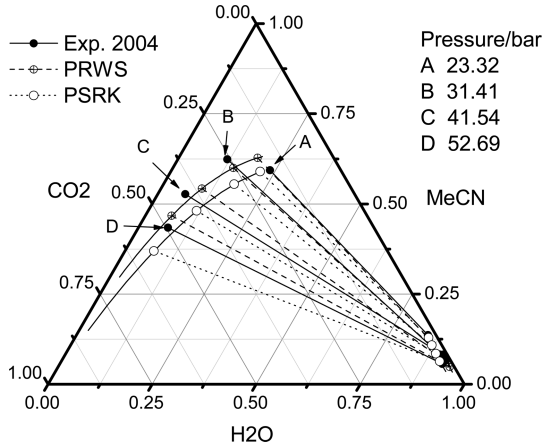

Figure A4. Triangle diagram of H_2O + MeCN + CO_2 ternary system at 313 K. Data reference 16, pressure range: 24−74 bar for PRWS and 25−70 bar for PSRK.

24 and 74 bar). In addition, PSRK was used to predict the phase behavior for comparison purposes due to its fully predictive character. Obviously, the profile of the liquid phase rich in MeCN stays below the experimental data, and the tie-lines feature larger deviations than the results of the PRWS model, especially when the pressure increases up to 50 bar. Thus, PRWS shows a better performance for predicting this system compared to PSRK.

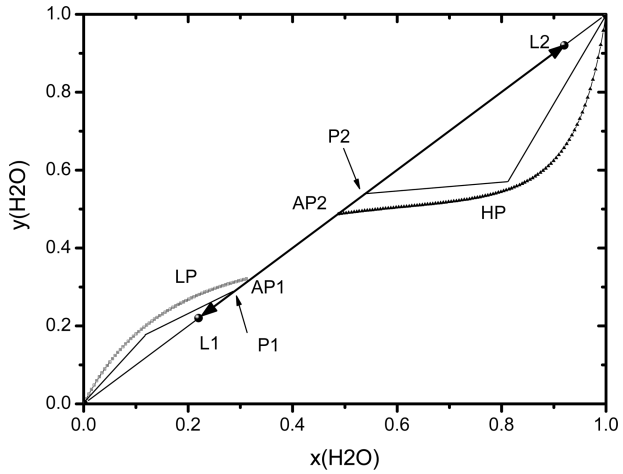

Figure A5. Operation of process variant 1 in a y−x diagram.

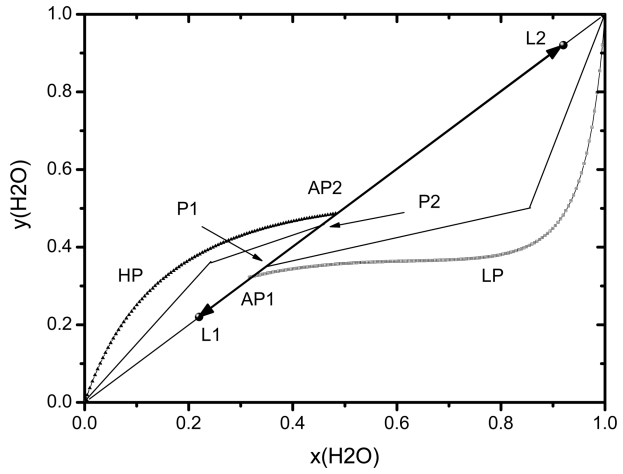

Figure A6. Operation of process variant 2 in a y−x diagram.

APPENDIX C. OPERATION OF PROCESSES IN Y−X DIAGRAMS

The operation of process variants 1 and 2 in a y−x diagram are shown in Figures A5 and A6.

AUTHOR INFORMATION

Corresponding Author

*Phone: +49 391 6110 350. Fax: +49 391 6110 634. E-mail: freund@mpi-magdeburg.mpg.de.

Notes

The authors declare no competing financial interest.

ACKNOWLEDGMENTS

K.Y. acknowledges financial support from the International Max Planck Research School for Analysis Design and Optimization in Chemical and Biochemical Process Engineering (IMPRS), Magdeburg, Germany.

SYMBOLS

x = mole fraction of liquid composition
y = mole fraction of vapor composition
i, j = component
k_{ij} = interaction parameter
T_c = critical temperature
P_c = critical pressure
ω = acentric factor
R, Q = UNIFAC parameter

ABBREVIATIONS

AP = azeotropic point
CO_2 = carbon dioxide
CEoS = cubic equation of state
EoS = equation of state
HP = high pressure
H_2O = water
IG = ideal gas model
LCSP = lower critical solution pressure
LP = low pressure
MeCN = acetonitrile
NRTL = non-random two liquids model
PSD = pressure-swing distillation
PSRK = predictive Soave−Redlich−Kwong
PR = Peng−Robinson EoS
UCSP = upper critical solution pressure
VLE = vapor−liquid equilibrium
VLLE = vapor−liquid−liquid equilibrium
WS = Wong−Sandler mixing rule

REFERENCES

(1) Baker, L. C. W.; Anderson, T. F. Some phase relationships in the 3-component liquid system CO_2-H_2O-C_2H_5OH at high pressures. *J. Am. Chem. Soc.* **1957**, *79*, 2071−2074.
(2) Elgin, J. C.; Weinstock, J. J. Phase equilibrium at elevated pressures in ternary systems of ethylene and water with organic liquids. Salting out with a supercritical gas. *J. Chem. Eng. Data* **1959**, *4*, 3−12.
(3) Adrian, T.; Wendland, M.; Hasse, H.; Maurer, G. High-pressure multiphase behaviour of ternary systems carbon dioxide water polar solvent: Review and modeling with the Peng-Robinson equation of state. *J. Supercrit. Fluids* **1998**, *12*, 185−221.

(4) Jessop, P. G.; Subramaniam, B. Gas-expanded liquids. *Chem. Rev.* **2007**, *107*, 2666−2694.
(5) Horizoe, H.; Tanimoto, T.; Yamamoto, I.; Kano, Y. Bench plant-test and process for the separation of ethanol-water solution using super-critical and subcritical propane solvent-extraction. *J. Chem. Eng. Jpn.* **1993**, *26*, 490−492.
(6) Adrian, T.; Freitag, J.; Maurer, G. High pressure multiphase equilibria in aqueous systems of carbon dioxide, a hydrophilic organic solvent and biomolecules. *Fluid Phase Equilib.* **1999**, *160*, 685−693.
(7) Adrian, T.; Freitag, J.; Maurer, G. A new high-pressure liquid-liquid extraction process for natural products recovery. *Chem. Eng. Technol.* **2000**, *23*, 857−860.
(8) Adrian, T.; Freitag, J.; Maurer, G. A novel high-pressure liquid-liquid extraction process for downstream processing in biotechnology: Extraction of cardiac glycosides. *Biotechnol. Bioeng.* **2000**, *69*, 559−565.
(9) Repke, J. U.; Forner, F.; Klein, A. Separation of homogeneous azeotropic mixtures by pressure swing distillation - Analysis of the operation performance. *Chem. Eng. Technol.* **2005**, *28*, 1151−1157.
(10) Modla, G.; Lang, P. Feasibility of new pressure swing batch distillation methods. *Chem. Eng. Sci.* **2008**, *63*, 2856−2874.
(11) Seader, J. D.; Henley, E. J. *Separation Process Principles*, 1st ed.; John Wiley & Sons, Inc.: New York, 1998.
(12) Huang, K. J.; Shan, L.; Zhu, Q. X.; Qian, J. X. Adding rectifying/stripping section type heat integration to a pressure-swing distillation (PSD) process. *Appl. Therm. Eng.* **2008**, *28*, 923−932.
(13) Matsuda, K.; Huang, K. J.; Iwakabe, K.; Nakaiwa, M. Separation of binary azeotrope mixture via pressure-swing distillation with heat integration. *J. Chem. Eng. Jpn.* **2011**, *44*, 969−975.
(14) Repke, J. U.; Klein, A. Homogeneous azeotropic pressure swing distillation: Continuous and batch process. *Comput.-Aided. Chem. Eng.* **2005**, *20*, 721−726.
(15) Repke, J. U.; Klein, A.; Bogle, D.; Wozny, G. Pressure swing batch distillation for homogeneous azeotropic separation. *Chem. Eng. Res. Des.* **2007**, *85*, 492−501.
(16) Lazzaroni, M. J.; Bush, D.; Jones, R.; Hallett, J. P.; Liotta, C. L.; Eckert, C. A. High-pressure phase equilibria of some carbon dioxide-organic-water systems. *Fluid Phase Equilib.* **2004**, *224*, 143−154.
(17) Ye, K.; Freund, H.; Sundmacher, K. Modelling (vapour-Liquid) and (vapour-Liquid-Liquid) equilibria of {water (H_2O)+methanol (MeOH)+dimethyl ether (DME)+carbon dioxide (CO_2)} quaternary system using the Peng-Robinson EoS with Wong-Sandler mixing rule. *J. Chem. Thermodyn.* **2011**, *43*, 2002−2014.
(18) Ye, K.; Freund, H.; Xie, Z.; Subramaniam, B.; Sundmacher, K. Prediction of multicomponent phase behavior of CO_2-expanded liquids using CEoS/GE models and comparison with experimental data. *J. Supercrit. Fluids* **2012**, *67*, 41−52.
(19) Eckert, C. A.; Knutson, B. L.; Debenedetti, P. G. Supercritical fluids as solvents for chemical and materials processing. *Nature* **1996**, *383*, 313−318.
(20) DeSimone, J. M. Practical approaches to green solvents. *Science* **2002**, *297*, 799−803.
(21) Leitner, W. Supercritical carbon dioxide as a green reaction medium for catalysis. *Acc. Chem. Res.* **2002**, *35*, 746−756.
(22) Maslan, F. D.; Stoddard, E. A. Acetonitrile-Water Liquid-Vapor Equilibrium. *J. Phys. Chem.* **1956**, *60*, 1146−1147.
(23) Blackford, D. S.; York, R. Vapor-Liquid Equilibria of System Acrylonitrile-Acetonitrile-Water. *J. Chem. Eng. Data* **1965**, *10*, 313−318.
(24) Gmehling, J.; Onken, U.; Arlt, W.; Grenzheuser, P.; Weidlich, U.; Kolbe, B.; Rarey, J. *Vapor-liquid equilibrium data collection, chemistry data series, DECHEMA. Part 1: Aqueous-Organic Systems*; DECHEMA: Frankfurt am Main, Germany, 1991.
(25) Acosta, J.; Arce, A.; Rodil, E.; Soto, A. A thermodynamic study on binary and ternary mixtures of acetonitrile, water and butyl acetate. *Fluid Phase Equilib.* **2002**, *203*, 83−98.
(26) Horstmann, S.; Jabloniec, A.; Krafczyk, J.; Fischer, K.; Gmehling, J. PSRK group contribution equation of state: comprehensive revision and extension IV, including critical constants and alpha-function parameters for 1000 components. *Fluid Phase Equilib.* **2005**, *227*, 157−164.